The recent Indian nuclear tests – A seismic overview

S. K. Sikka*, G. J. Nair, Falguni Roy, Anil Kakodkar and R. Chidambaram

Seismology Division, Solid State and Spectroscopy Group, Bhabha Atomic Research Centre, Mumbai 400 085, India

This paper reviews the seismic analysis of the close-in, regional and teleseismic data corresponding to May 1998 Indian nuclear tests. Strong Lg and Rayleigh waves (period 3.5–7 s) were observed at several in-country stations from the two large explosions of 11 May 1998 (POK2). The magnitude of POK2 based on regional Lg wave data was obtained as 5.47 ± 0.06. A comparison of Lg waves at Gauribidanur array (GBA), India corresponding to POK2 with that of the Indian explosion of May 1974 (POK1) gave a yield ratio of 4.83 between these events, which is very near to the value of 4.46 obtained from the differences in m_b values between POK2 and POK1. Analysis of regional Rayleigh waves provided a M_s value of 3.56 for POK2 and also revealed that Nuttli's relation for estimation of surface wave magnitude based on eastern North American data is also applicable to Indian region. The yield estimates of POK2 from the teleseismic, regional and close-in seismic data, were found to be consistent with those obtained from the post-shot radio-chemical measurements. The analysis of spectrograms generated from seismograms of POK2 and Pakistan explosion of 28 May 1998 showed that the ratio of source energies between these events is higher than what was obtained from global m_b values.

Introduction

At the Pokhran test site in Rajasthan, India, five underground nuclear tests were carried out by India during 11–13 May 1998. Three explosives were detonated simultaneously on 11 May (POK2). These consisted of a thermonuclear device (45 kt), a fission device (15 kt) and a subkiloton (less than one kiloton) device emplaced in three different shafts. The two simultaneous tests carried out in two separate shafts on 13 May 1998 were also of subkiloton type. The yields of all the explosions were announced by India immediately after these tests. It is satisfying that analysis of close-in seismic data of these explosions as well as that of global teleseismic and regional seismic data confirms these yields[1–4].

The prototype International Data Centre (pIDC) for verifying the compliance of Comprehensive Test Ban Treaty (CTBT), surprisingly identified the 11 May tests initially as an earthquake from the India–Pakistan border. The 13 May tests[5] were reported as not detected by the pIDC, which indicates that the present detection threshold of the pIDC may be above 1 kt for the Pokhran region which is higher than the detection threshold (< 1 kt) recommended for IDC[6]. Regarding the yield estimates of the 1998 Indian nuclear explosions, while some seismologists around the world have estimated the total yield of 11 May tests near to the announced yield[7] of 60 kt, some other seismologists have given much lower estimates[8,9]. The under-estimation of the yield can be attributed to the use of data from simultaneous spatially separated explosions without incorporating necessary corrections for source geometry and to the ad hoc assumptions used in the estimation of the yield from body waves.

Nuclear seismology

An underground nuclear explosion sets up a shock wave near the point of detonation which interacts with the surrounding geological medium. This shock wave vaporizes, melts, plastically deforms and fractures the surrounding rocks and then degenerates into elastic waves. Only a small portion of the total energy released by an underground explosion is converted into seismic waves. The ratio of the elastic wave energy to the total energy is known as seismic efficiency. The seismic efficiency depends on the physical characteristics of the surrounding medium and the source parameters. The seismic waves produced by an underground explosion travel through the body of the earth as well as along its surface. The waves that propagate through the body of the earth are called body waves which comprise compressional P waves and shear S waves. At short distances (up to ~ 2000 km) from the source the path of the body waves is through the crust and top portion of upper mantle and these waves are known as regional seismic waves. The waves observed beyond ~ 2000 km which travel through the fairly homogeneous mantle and the core, are termed as teleseismic waves. Theoretically, in an isotropic medium, P waves travel with a velocity $\sqrt{3}$ times that of the S waves and the frequency content of P waves is usually higher than that of S waves.

Among surface waves, two groups of waves, viz. Rayleigh (R) waves, with vertical elliptic particle motion

*For correspondence. (e-mail: sksikka@magnum.barc.ernet.in)

along the direction of wave propagation and the Love (L) waves, with horizontally polarized shear motion perpendicular to the direction of propagation are seen prominently at regional distances. The period of R waves varies from ~ 3 s to 200 s. At regional distances, higher mode Love and Raleigh waves, called Lg waves, form strong group of arrivals before the fundamental mode Love waves with an average velocity of ~ 3.5 km/s. The short period Lg waves from explosions are predominant in the frequency band of 0.2 to 1 Hz and have in general large amplitudes among the regional phases.

Seismologists measure the energy of seismic sources, viz. explosions or earthquakes, using a magnitude scale. Empirically, magnitude (m) is defined as the logarithm of the ratio of the ground displacement amplitude (A) in micron and time period (T) of a particular wave added with a distance correction factor $B(\Delta)$ accounting for the attenuation and geometrical spreading of the wave with distance Δ in degree. It is expressed as

$$m = \log(A/T) + B(\Delta). \quad (1)$$

Three magnitude scales are most often used. They are the body wave magnitude, m_b, the surface wave magnitude, M_s, and Lg wave magnitude, m_b(Lg). For body waves, distance correction factor, $B(\Delta, h)$, where h is depth of the source, can be obtained from the tables of Veith and Clawson[10] or Gutenburg[11]. For surface waves of periods ~ 10 s or more, $B(\Delta) = 3.3 + 1.66 \log(\Delta)$ (ref. 12) and $B(\Delta) = 2.6 + 1.66 \log(\Delta)$ (ref. 13) for 3–12 s surface waves associated with airy phase. The distance correction term for guided Lg waves of period 1 s, is given by $B(\Delta) = 3.81 + 0.83 \log(\Delta) + \gamma(\Delta - 0.09) \log(e)$ (ref. 14), where γ is a path-dependent constant.

A modified body wave magnitude termed as m_Q, which incorporates the correction for the upper mantle attenuation effects at the explosion source site as well as at the receiver site and for the depth of explosion, was developed by Marshall *et al.*[15]. This is given by

$$m_Q = m_b + RC(T) + SC(T) + DC(T). \quad (2)$$

Here RC, SC and DC are the receiver site, source site and the depth correction factors respectively, which are functions of the time period T of the P signal. Using these derived m_Q values for a large number of nuclear explosions, Marshall *et al.*[15] fitted a linear regression relation for the m_Q versus logarithm of yield which gives a lower scatter compared to m_b-logarithm of yield relation.

The yield of a nuclear explosion is calculated from an empirical relation between yield Y, in kt and the magnitude m given by

$$m = C1 + C2 \log Y, \quad (3)$$

where C1 and C2 are constants specific to the testing site. Therefore, for determining the yield of an explosion, one has to first estimate the magnitude and then use site-specific values of C1 and C2 in relation (3).

Coming to the m_b versus yield formulae, it may be pointed out that such relations are available only for a few well-known testing sites of nuclear-weapon states. It is seen that while C1 is test-site dependent, C2 varies in a narrow range of 0.75 to 0.85 (ref. 16). Arbitrary use of C1 value of a known test site for an unknown site may be inappropriate as the efficiency of coupling of energy of explosion to the surrounding earth depends upon the geophysical properties of the rocks in the immediate vicinity of the explosion site. Significant change in C1 value may occur even over small distance as may be seen from the example of test sites at the former Soviet Shagan river and Degelen[17]. The variation of C1 value from region to region could be attributed to differences in porosity and strength of the rocks in the immediate vicinity of the explosion site. To illustrate this, a rock mechanics calculation of reduced displacement potential (RDP, a measure of seismic signal strength) for similar rocks with 5% porosity difference is shown in Figure 1 which gives a difference of magnitude of 0.3 (refs 18, 19). In this context it may be pointed out that the use of former Soviet Shagan River site parameters for Pokhran site by some US seismologists[8] is not justified.

The network averaged spectra corrected for medium, source and instrument effects[20] and synthesis of seismograms to match observed seismograms[21] are also employed for estimating source parameters of explosions. However these methods use only P wave portion of the seismic data and have to be supplemented with analysis of regional seismic data (comprising P, Lg and Rayleigh waves) as well as close-in data like ground acceleration.

Body wave magnitude for simultaneous explosions

It may be noted that due to anisotropy and heterogeneities in the earth, the order of variation of m_b values observed

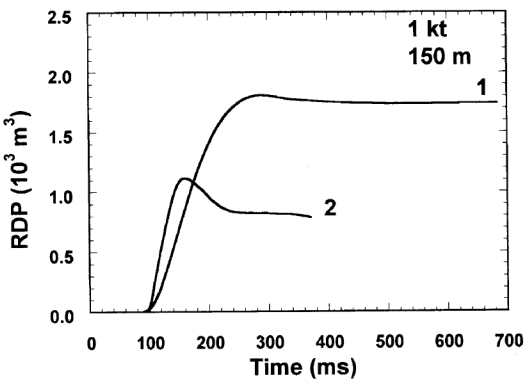

Figure 1. Calculated RDPs for 1 kt explosion in two rocks of same type with different porosity. The curve 2 is for rocks with porosity of 5%.

at different seismic stations from a given explosion may be as high as one magnitude unit. In practice, the magnitude of an event is obtained by averaging all the globally measured magnitude values. This procedure assumes that errors in magnitudes, due to differences in propagation path characteristics from source to different seismic stations, are random. This procedure of computing average m_b requires further correction if explosions are carried out simultaneously similar to the 11 May 1998 Indian explosions as it does not account for the destructive interference effect of *P*-wave signals emanating from the individual explosions. One way of overcoming this problem is to follow a method suggested by Sikka *et al.*[2] which uses the source geometry and synthetic seismograms to correct the global magnitude estimates. With the help of synthetic seismograms it was demonstrated that due to the interference of the *P* signals from the two large explosions of POK2, the values of m_b along the line joining the two explosion sites would be less by about 0.3 magnitude units for a t^* value (ratio of *P* wave travel time to average *Q* value on the path from source to receiver) of 0.4 s. The revised m_b estimate of POK2 was subsequently obtained as 5.4.

Estimation of m_b(Lg) from regional Lg wave data

The seismic Lg wave as described earlier, is one of the many regional phases that propagates in the continental lithosphere. In general, for a given event, the amplitude of Lg phase at regional distances is larger than *P* and *S* phases for the continental paths. Due to the isotropic nature of Lg wave radiation pattern, a reliable magnitude determination can be made from the data of only a small number of stations[13,22]. Thus Lg signals provide an excellent basis for estimating yields of nuclear explosions even down to below 1 kt, when such signals are recorded at high quality digital, in country seismic stations, and when calibrated by access to independent yield information for a few nuclear explosions at the test sites of interest.

Since Lg represents a higher mode surface wave traveling with minimum group velocity, it would be appropriate to relate Lg wave amplitude (A) and distance (Δ) as,

$$A = K \cdot \Delta^{-1/3} (\sin(\Delta))^{-1/2} \exp(-\gamma\Delta), \quad (4)$$

which is the expression for the amplitude of dispersed surface waves measured in the time domain corresponding to the Airy phase[13]. In expression (4), K is a constant governed by the source strength and γ is the anelastic attenuation coefficient which is related to specific quality factor $Q = \pi/UT\gamma$, where U is the group velocity and T is the period of the wave. In order to obtain the value of m_b(Lg) it is necessary to determine γ for a particular source receiver path. Having estimated γ, m_b(Lg) can be obtained from the relation[14],

$$m_b(\text{Lg}) = 3.81 + 0.83 \log(\Delta) + \gamma(\Delta - 0.09) \log(e) + \log(A), \quad (5)$$

where A corresponds to Lg amplitude in microns at signal periods close to 1 s.

Figure 2 *a* shows the broad band seismogram as recorded at Bhopal observatory (BHPL) of the India Meteorological Department (IMD), India. Clear Lg and Rayleigh waves with high signal to noise ratio (SNR) are seen in the seismogram. On the other hand, the seismogram of the Nilore station in Pakistan (NIL, an international monitoring station situated in Himalayas at a similar distance $\Delta = 6.67°$ from the POK2 site compared to BHPL $\Delta = 6.34°$), shows highly attenuated Lg waves (see Figure 2 *b*). It is thus evident that Lg wave attenuation along the path between NIL and POK2 site is much higher than that along the path between BHPL and POK2 site. The average m_b(Lg) value of POK2 from the data of four Indian stations is obtained as 5.47 (Table 1) with a standard deviation of 0.06 (ref. 4). It may be noted that the Trivandrum observatory (TRVM, $\Delta = 19.12°$) of the IMD recorded strong Lg waves of ~ 4 s period on long period seismograms[4]. As the short period data from TRVM are not available, determination of m_b(Lg) using 1 s period Lg wave could not be done. Nevertheless, the amplitude of 4 s period Lg wave is apparently consistent with the average m_b(Lg) estimate as obtained from other four stations data. However, the Ajmer observatory (AJM, $\Delta = 2.57°$) of the IMD recorded somewhat attenuated Lg waves compared to the other five stations. This implies that the path between the POK2 site and AJM is charac-

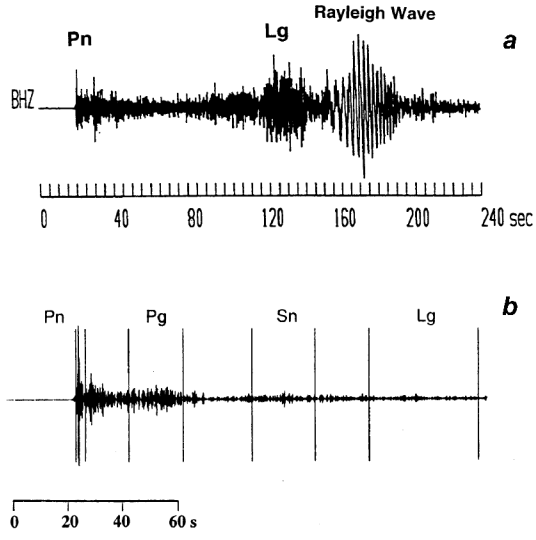

Figure 2. *a*, Broad-band seismogram corresponding to POK2 as recorded at BHPL, India; *b*, Seismogram generated by POK2 at NIL, Pakistan[34]. High attenuation of Lg waves on NIL record in comparison to that on BHPL record is conspicuously seen.

terized by a higher γ value than that of the other five stations. This could be due to the proximity of AJM to the Aravali ranges. Figure 3 shows strong Lg waves on the short period seismogram of GBA, India. From GBA data the amplitude ratio of Lg waves between POK2 and that of Indian explosion of 18 May 1974 (POK1) at 1 s period is obtained as 3.7, which gives the difference in magnitudes ($\Delta\, m_b$(Lg)) between these two events as 0.57.

Estimation of m_b(Lg) of POK2 from a relation based on regional earthquake data

A recent study[23] using the GBA data pertaining to 23 earthquakes from the Indian subcontinent revealed that the Lg was the most prominent among the regional phases and had the largest amplitude irrespective of the event magnitudes and epicentral distances. The excellent stability of the magnitudes based on the RMS Lg from underground nuclear explosions was demonstrated earlier by Hansen *et al.*[24]. In view of the above, a regional magnitude scale based on the RMS value of the Lg waves at GBA has been developed by Bhadauria *et al.*[23] which was derived from the data of 23 regional earthquakes ($3.8 \le m_b$ (USGS) ≤ 5.4) in the distance range from 3.34° to 18.92°. The estimated m_b(Lg) values using this relation were found to have very close agreement with the USGS reported m_b values for these events. For seven events with m_b (USGS) ≥ 5.0, a linear fit between the USGS m_b values and the m_b(Lg) estimates[23] gave a relation m_b(Lg) = m_b (USGS) $\pm$ 0.07. However, for the events with m_b (USGS) < 5.0, the relation, m_b(Lg) = m_b (USGS) $\pm$ 0.20 was obtained. Using the RMS Lg-based relation[23], the m_b(Lg) value of POK2 is obtained as 5.43. This is in excellent agreement with the m_b(Lg) value of 5.42 obtained earlier[4] from GBA data (Table 1). It may be interesting to note that the same relation gave the m_b(Lg) estimate of recent Chamoli earthquake (Northern India, 28 March 1999) as 6.39, showing excellent agreement with the USGS determined m_b of 6.4 for this event.

Determination of M_s from regional Rayleigh wave data

For POK2 there were only four teleseismic M_s observations available compared to 160 observations corresponding to m_b as reported by the USGS, the pIDC and Kyrgiz network (KNET). However, at the regional distances ($\Delta < 2000$ km), Rayleigh waves in the period range 3.5 s–7.0 s with high SNR have been observed at several Indian stations. Similar observation was made by Nuttli[13] in his study of central US earthquakes where, for one of the events, Rayleigh waves of 3–12 s period at regional distances yielded M_s values as high as 4.08 but no teleseismic surface wave of 20 s period was seen. The average surface wave magnitude for POK2 using the four teleseismic observations of the USGS (KEV, KONO, HAU and FLN) is obtained as 3.57. Using this value of M_s = 3.57 and the regional data from six stations corresponding to POK2 having signal periods between 3.5 s and 7.0 s, a relation for M_s is obtained as[4]

$$M_s = 2.75 + 1.51 \log(\Delta) + \log(A/T)_{max}. \quad (6)$$

For regional distances between 2° and 20°, Nuttli[13] has proposed the formula for vertical component of Rayleigh waves having periods between 3 and 12 s as

$$M_s = 2.6 + 1.66 \log(\Delta) + \log(A/T)_{max}, \quad (7)$$

where Δ is in degrees and $(A/T)_{max}$ is the maximum value of A/T in microns per second. The M_s estimates obtained using these two relations ((6) and (7)) are listed in Table 2. It may be seen that both the relations give M_s estimates close to each other. Nuttli's relation gives an average M_s value of 3.56. The values of standard deviations for M_s (ref. 4) and M_s (Nuttli) are obtained as 0.259 and 0.263 respectively. As the difference between these standard deviations is negligible, we conclude that Nuttli's relation, which has been derived from the data of some independent events, is applicable for the Indian region as well.

Table 1. Estimates of m_b(Lg) from regional data

Station code/name	Distance (°)	Azimuth (°)	m_b(Lg)
BHPL/Bhopal	6.34	126.1	5.43
POO/Pune	8.73	167.4	5.46
BLSP/Bilaspur	10.58	115.7	5.57
GBA/Gauribidanur	14.41	157.7	5.42

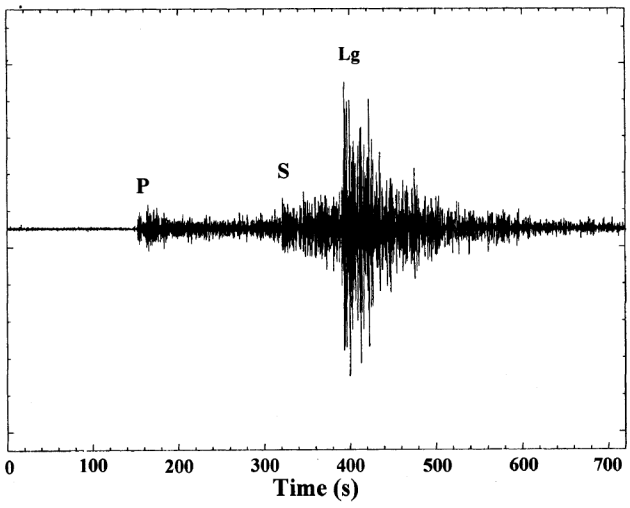

Figure 3. Short-period seismogram of GBA corresponding to POK2 showing strong Lg waves.

Comparison of spectrograms of POK2 and 28 May 1998 explosion of Pakistan

The running spectrograms of seismic events as a three dimensional (time, frequency and amplitude) representation of seismic wave energy reaching a recording station give detailed insight into the source function and the event signatures. The spectrograms shown in this paper are generated by an in-house developed software which filters the time series through multiple narrow band filters with defined center frequency increments[25]. The spectrogram of POK2 from BHPL ($\Delta = 6.34°$) seismogram is shown in Figure 4. The different signal arrivals, viz. *P*, *S*, Lg and *R* waves along with some higher modes are prominently seen in the spectrogram. The Rayleigh wave energy peaks at a period ~ 4 s while the Lg waves show predominant energy in the frequency band around 1 Hz. The spectrograms of Pakistan explosion of 28 May 1998 (PAK1) generated from seismograms of BHUJ ($\Delta = 7.21°$) and AJM ($\Delta = 9.09°$) are shown in Figures 5 and 6 respectively. The arrivals seen in these spectrograms show that at this distance range (6° to 9°) the low frequency energy for Pakistan explosion is much smaller than that of POK2. The spectrogram at AJM shows that this feature of lower amount of low frequency energy in Pakistan explosion is not specific to the BHUJ data but also seen in the data of many other stations. Also, the comparison of energy in Rayleigh and Lg phases, between POK2 and PAK1 shows that the ratio of the source ener-

Table 2. Estimates of M_s from regional data

Station code/name	Distance (°)	Azimuth (°)	M_s (Nuttli)	M_s (Present authors)
AJM/Ajmer	2.57	103.4	3.32	3.41
BHPL/Bhopal	6.34	126.1	4.00	4.03
POO/Pune	8.73	167.4	3.20	3.21
BLSP/Bilaspur	10.58	115.7	3.74	3.74
GBA/Gauribidanur	14.41	157.7	3.55	3.53
TRVM/Trivandrum	19.12	164.4	3.54	3.50

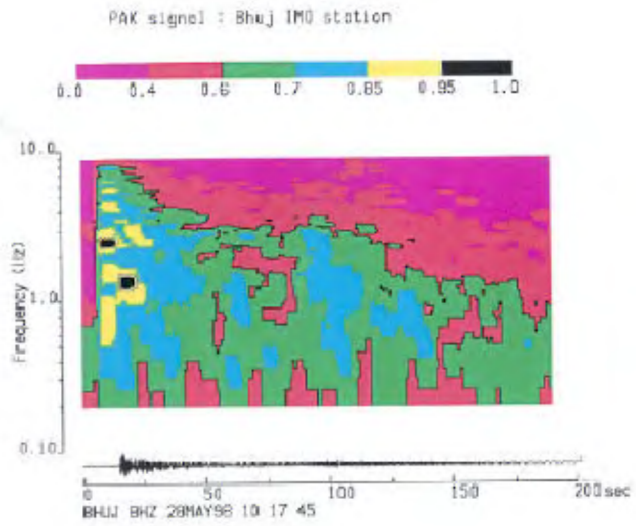

Figure 5. Spectrogram of Pakistan explosion of 28 May 1998 generated from the broad-band seismogram of BHUJ ($\Delta = 7.21°$). Nomenclatures are as in Figure 4.

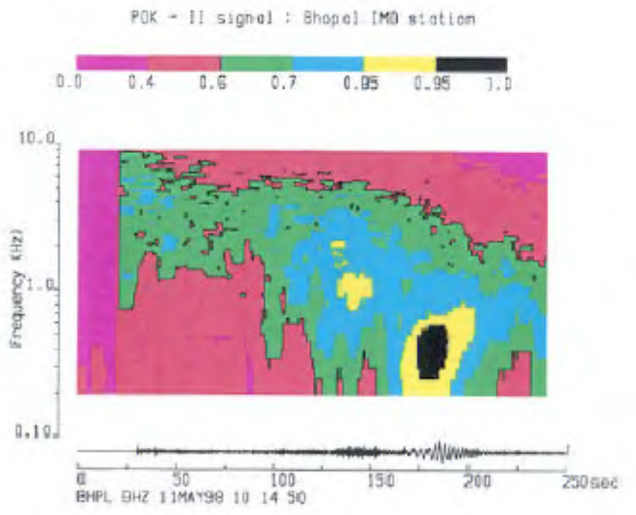

Figure 4. Spectrogram of POK2 generated from the broad band seismogram of BHPL ($\Delta = 6.34°$). The seismogram is shown at the bottom. The normalized logarithmic spectral amplitudes are shown at the top.

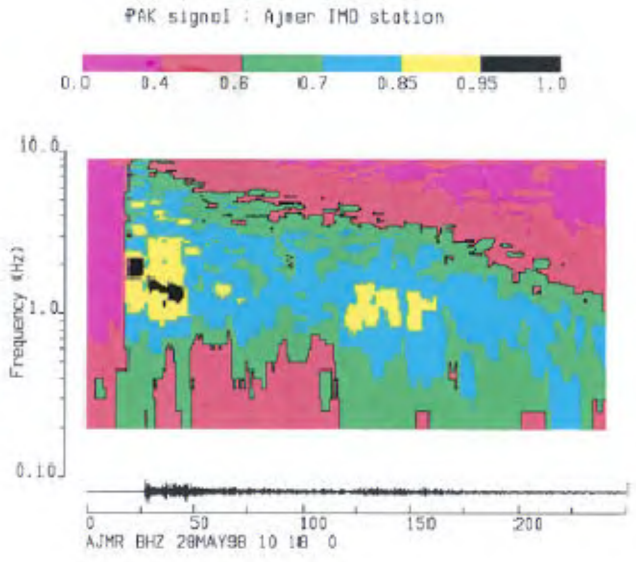

Figure 6. Spectrogram of Pakistan explosion of 28 May 1998 generated from the broad-band seismogram of AJM ($\Delta = 9.09°$). Nomenclatures are as in Figure 4.

gies between these events is much larger than that obtained from the global m_b reported by USGS.

Seismic yield of POK2

Yield of POK2 was obtained by comparing m_b values of POK1 and POK2 from eight stations around the world[3], which recorded P waves from both these explosions, and also by comparing the Lg amplitudes of these explosions as recorded at GBA. A reliable estimate of the yield ratio ΔY between the two explosions can be obtained from equation (3) using relation $\Delta m_b = C2 \log(\Delta Y)$, where Δm_b is the difference in m_b between the events. For the Pokhran region, the value of C2 is obtained as 0.77 (ref. 2). The average Δm_b between POK2 and POK1 for eight stations is obtained as ~ 0.5 (ref. 3) which gives a yield ratio ΔY of about 4.46. A comparison of P waveforms corresponding to POK2 and POK1 recorded at GBA is shown in Figure 7. Using the announced yield of 12–13 kt (refs 26, 27) for POK1, which reproduced many post-shot experimental data[18] like measured cavity radius, surface velocity and the extent of rock fracturing using rock mechanics phenomenology calculations, and also accepted internationally by many seismologists[15,28], one gets the yield, Y, for POK2 as $54 < Y < 58$ kt, very close to the value (58 to 63 kt) obtained from the m_b(Lg) estimates of the two explosions as recorded at GBA[4].

Yield values of an explosion based on long period surface waves generally show less scatter than those based on short period data, provided there are sufficient number of surface wave records. The wavelengths of the surface waves are considerably longer than those of the P waves and therefore they are less influenced by small scale heterogeneities along the path as well as interference effects produced by closely spaced simultaneous explosions. From the estimated M_s value, 3.56, of POK2 explosions[4], and employing the M_s-yield relation of Murphy[29]

$$M_s = 2.14 + 0.84 \log(Y) \quad (8)$$

which is applicable to explosions with yield less than 100 kt, we get the yield of POK2 as 49 kt. However, using the relation of Evernden and Marsh[30] the yield is obtained as 52 kt. These estimates are found to be in agreement with the yields derived from the body wave and Lg wave magnitudes.

Discussion

The m_b value of 5.4 for POK2 (ref. 2) obtained by taking into account the source geometry, was close to the estimated m_b(Lg) value[4] for these explosions. These put the yield of POK2 in the range of 54–63 kt. Surface wave magnitude of POK2 is obtained as 3.56 from the regional data which corresponds to an yield of 49–52 kt. We have also computed m_Q for POK2 using equation (2). For estimating source and receiver site corrections we have used the relationship between the body wave attenuation in the upper mantle and Pn velocity as given by Marshall *et al.*[15]. It may be noted that the Pokhran site is a part of the Western Ganga Basin, where the crustal block has been classified by seismologists (e.g. Chun[31]) as having oceanic affinity. Using a Pn velocity of 8 km/s for this region, the source correction works out to be 0.16. A modified m_Q derived from stations with known receiver corrections was obtained as 5.80, after taking into account corrections due to source geometry. This m_Q value is plotted for an yield of 58 kt in Figure 8 along with the data of Marshall *et al.*[15] for other nuclear tests. Both POK2 and POK1 yield estimates agree well with the global trend.

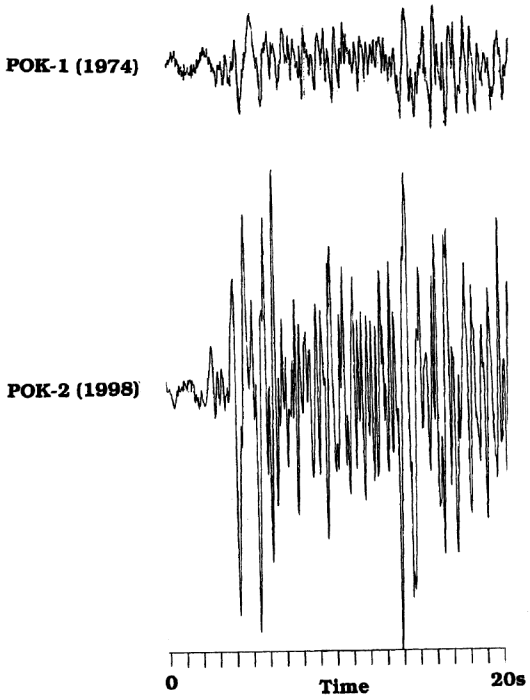

Figure 7. Short period P waveforms of POK1 and POK2 as recorded at GBA.

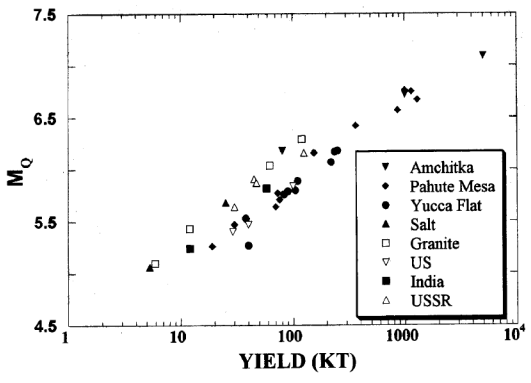

Figure 8. The plot of M_Q versus yield of some explosions in hard rock[15] along with POK2 data.

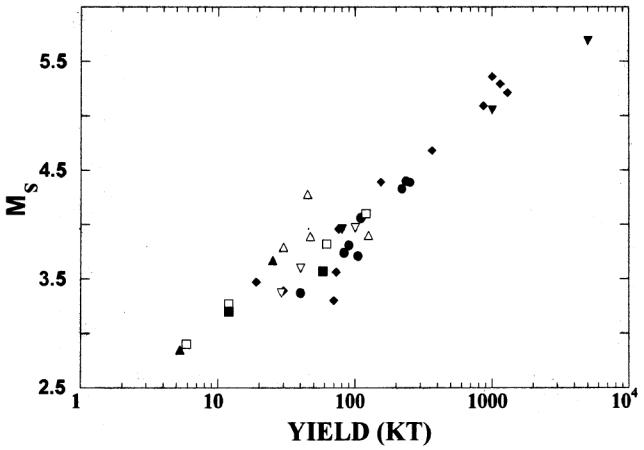

Figure 9. A plot of M_S versus yield for explosions in hard rock[15] along with POK2 data. The definitions of symbols are same as in Figure 8.

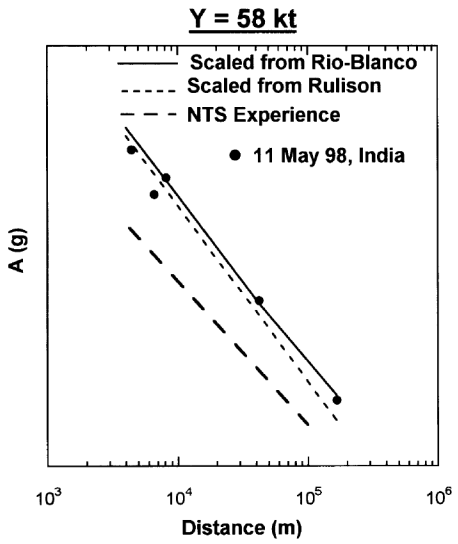

Figure 10. Measured accelerations for POK2 compared to some US tests scaled for an yield of 58 kt.

Doubts have been raised especially by Wallace[9], based on some unconfirmed reports, about the yield of POK1 explosion and the use of scaling between the surface crater produced and the depth of burial. It may be pointed out that the surface features produced by an underground explosion are heavily dependent upon the geo-physical properties of rock medium in the vicinity of the explosion and which may also vary from place to place even in the same testing range. It may be reiterated here that Chidambaram *et al.*[18] have explained the post-shot experimental data of POK1 by rock mechanics calculations employing measurements of the physical properties of Pokhran rocks. It may also be noted that yields of POK2 based on global and regional M_S estimates are derived independent of POK1 yield. Further, the M_S-yield data of POK2 is found consistent with the trend of M_S-yield data of a large number of global explosions reported by Marshall *et al.*[15] and Bache[28] (see Figure 9).

It is well known that the yield of a nuclear explosion can be determined with a reasonable accuracy from the close-in acceleration and velocity measurements. Comparison of the close-in seismic data pertaining to POK2 with the available global data from similar geophysical environment gives an yield value close to 58 kt for these explosions (see Figure 10)[3]. Recent radiochemical analysis of samples from post-shot logging of POK2[32] has confirmed the authenticity of the estimated seismic yields of POK2 explosions. The radiochemical yield for the thermonuclear device has been obtained as 50 ± 10 kt. A preliminary estimate of the radiochemical yield of the fission device, is 13 ± 3 kt (ref. 33). These studies have further substantiated that the fusion component was in accord with computer simulations. The yields of the sub-kiloton devices which were derived from some close-in measurements have also been proven correct by radiochemical analysis[5]. It may be added that Barker *et al.*[8] have given a detection threshold of m_b(Lg) of 2.5 at Nilore (NIL) in Pakistan for the events in Pokhran region. Based on their yield estimate for 11 May 1998 tests as 9–16 kt, they put the yield of 13 May explosions between 30 and 300 tons. With the actual yield ~ 60 kt for 11 May tests this detection limit will be in the range 0.1 to 1 kt.

To conclude, it is clear from the above that yield of POK2 obtained by employing different methods are close to 60 kt, and are in agreement with the announced yields[1].

1. Sikka, S. K. and Kakodkar, Anil, *BARC News Lett.*, 1998, **172**, 1–4.
2. Sikka, S. K., Roy, F. and Nair, G. J., *Curr. Sci.*, 1998, **75**, 486–491.
3. Sikka, S. K., Roy, F., Nair, G. J., Kolvankar and Kakodkar, Anil, *BARC News Lett.*, 1998, **178**, 1–5.
4. Roy, F., Nair, G. J., Basu, T. K., Sikka, S. K., Kakodkar, A., Chidambaram, R., Bhattacharya, S. N. and Ramamurthy, V. S., *Curr. Sci.*, 1999, **77**, 1669–1673.
5. Attarde, R. B., Shukla, V. K., Babu, D. A. R., Kulkarni, V. V. and Kakodkar, A., *BARC News Lett.*, 1999, **188**, 1–3.
6. Sullivan, J. D., *Physics Today*, March 1998, pp. 24–29.
7. Evernden, J. F., *Phys. Soc.*, 1998, **27**, 10–11.
8. Barker, B. *et al.*, *Science* 1998, **281**, 1967–1968.
9. Wallace, T. C., *Seismol. Res. Lett.*, 1998, **69**, 386–393.
10. Veith, K. F. and Clawson, G. E., *Bull. Seismol. Soc. Am.*, 1972, **62**, 435–451.
11. Gutenberg, B., *Bull. Seismol. Soc. Am.*, 1945, **35**, 57–69.
12. Dahlman, O. and Israelsson, H., *Monitoring Underground Nuclear Explosions*, Elsevier, Amsterdam, 1977.
13. Nuttli, O. W., *J. Geophys. Res.*, 1973, **78**, 876–885.
14. Herrmann, R. B., *Bull. Seismol. Soc. Am.*, 1980, **70**, 447–468.
15. Marshall, P. D., Springer, D. L. and Rodean, H. C., *Geophys. J. R. Astron. Soc.*, 1979, **57**, 609–638.

16. Chyba, C. F., van der Vink, G. E. and Hennet, C. B., *Geophys. Res. Lett.*, 1998, **25**, 191–194.
17. Nuttli, O. W., *Bull. Seismol. Soc. Am.*, 1987, **77**, 679–681.
18. Chidambaram, R., Sikka, S. K. and Gupta, S. C., *Pramana*, 1985, **24**, 245.
19. Gupta, S. C. and Sikka, S. K., 1998 (to be published).
20. Murphy, J. R., Barker, B. W. and O'Donnell, A., *Bull. Seismol. Soc. Am.*, 1989, **79**, 141–156.
21. Douglas, A., Hudson, J. A. and Blamey, C., *Geophys. J. R. Astron. Soc.*, 1972, **28**, 385–410.
22. Nuttli, O. W., *J. Geophys. Res.*, 1986, **91**, 2137–2151.
23. Bhadauria, Y. S., Roy, F. and Prasad, A. G. V., Workshop on Chamoli Earthquake and its Impact, WOCEI-99, WIHG, Dehradun, India, 1999.
24. Hansen, R. A., Ringdal, F. and Richards, P. G., *Bull. Seismol. Soc. Am.*, 1990, **80**, 2106–2126.
25. Basu, T. K., Roy, F., Roy, D. and Singh, M., Workshop on Chamoli Earthquake and its Impact, WOCEI-99, WIHG, Dehradun, India, 1999.
26. Nair, G. J., Some Seismic Results of Rajasthan Explosion of 18 May 1974, AG224, Procurement Executive, MOD, UK.
27. Chidambaram, R. and Ramanna, R., Proc. Tech. Committee on Peaceful Nuclear Explosions IV (Vienna, IAEA), 1975, p. 421.
28. Bache, T. C., *Bull. Seismol. Soc. Am.*, 1982, **72**, S131.
29. Murphy, J. R., *Bull. Seismol. Soc. Am.*, 1977, **67**, 135.
30. Evernden, J. F. and Marsh, G. E., *Physics Today*, August 1987, pp. 37–44.
31. Chun, K. Y., *Bull. Seismol. Soc. Am.*, 1986, **76**, 1687–1698.
32. Manohar, S. B., Tomar, B. S., Rattan, S. S., Shukla, V. K., Kulkarni, V. V. and Kakodkar, A., *BARC News Lett.*, 1999, **186**, 1–5.
33. Manohar, S. B. (private communication).
34. *Science and Technology Review*, LLNL, California, September, 1998, 4–11.

ACKNOWLEDGEMENTS. We thank Dr S. K. Srivastav and Dr S. N. Bhattacharya for providing the digital data of IMD stations used in this study. We also thank Mr T. K. Basu for providing the spectrograms of the events. Thanks are also due to our colleagues at Gauribidanur for giving the digital transcripts of data used.

Seed-mediated growth method to prepare cubic copper nanoparticles

Nikhil R. Jana[#], Zhong L. Wang[‡], Tapan K. Sau[**] and Tarasankar Pal[*,†]

*Department of Chemistry, Indian Institute of Technology, Kharagpur 721 302, India
[#]University of South Carolina at Columbia, SC, USA
[‡]Georgia Institute of Technology, Atlanta, GA, USA
**Chemistry Department, Panjab University, Chandigarh 160 014, India

A new and simple method has been reported here which can be applied to control simultaneously the shape and size of the copper nanoparticles, without using any capping agent or template. By this method, cube-shaped copper nanoparticles in the size range ~ 75–250 nm were formed from smaller spherical copper particles. At the first stage, 5–6 nm spherical copper particles were prepared from aqueous copper sulphate solution by borohydride reduction. In the second stage, these small particles were mixed with appropriate amount of copper sulphate and sodium ascorbate, which resulted in the production of larger size cubic copper particles. In the latter step, the new grown larger particles acted as seed and grew larger due to the reduction of copper ions by ascorbate ion on their surfaces. Thus cubic copper nanoparticles of varied size regime were produced by ascorbate ion by varying the ratio of copper seed particles to copper ion concentrations in solution.

METAL nanoparticles, due to their special properties and also small dimensions, find important applications in optical, magnetic, thermal, electronic and sensoric devices, SERS (surface enhanced Raman scattering), catalysis, etc.[1]. Almost all properties of nanoparticles are due to their small sizes[1–6]. Of late, in addition to size effect, shape of the particles has also drawn special attention, mainly to explore the application of these particles in the field of nanotechnology. Therefore, attempts are being directed to gain precise control of the size and the shape of various types of nanoparticle systems during their syntheses[7–15]. The fact is that these syntheses result in a mixture of particles, in terms of both size and shape. The most common method employed for their preparation is the reduction of metal ions in solution, usually in the presence of a particle-stabilizer[2,3,7]. However, the control of size and, particularly, the shape at the nanometre level is a real problem, as the mechanism of size/shape control is still left largely unresolved[8]. There are few general methods available for size control, and for shape control, these are very few. These methods use either a capping agent or a template for the restricted growth of the particles. Some people used a seed-mediated controlled growth to prepare particles of different sizes[16–18]. We exploited, for the first time, the seed-mediated method to prepare copper nanoparticles of cubic shape and variable size. To our knowledge, there is no simpler method of preparation reported that could yield simultaneously size- and shape-controlled nanoparticles at room temperature. Some reverse micelle-based template methods are available to control the copper particle size[19]. Reverse micelle has also been used to prepare nanosize rod-shaped copper particles[20]. Micrometre-size cubic copper particles were obtained by dissolving the spheres of basic copper carbonate which was formed by aging at 90°C a solution containing $Cu(NO_3)_2$ and urea, with the slow addition of $NH_2OH \cdot HCl$ into the solution[7].

An aliquot of 100 ml water solution of $CuSO_4$ (2×10^{-4} mol.dm^{-3}) was taken in a conical flask and purged with N_2 for 10 min to remove the dissolved oxygen. Then 1 ml ice-cold $NaBH_4$ (0.1 mol.dm^{-3}) solution was added into the $CuSO_4$ solution with stirring. The metal particles are formed immediately, visualized by the appearance of a yellow colour; for the quantitative confirmation, spectrophotometric investigation was made.

Appropriate amount (see Table 1 for conditions) of $CuSO_4$ was taken in water (final volume 100 ml) and the dissolved oxygen was removed by N_2 purging. The solution was then stirred with a magnetic stirrer. Then required amount of seed particles was mixed with this solution. Finally, ascorbic acid was added drop by drop. N_2 purging was continued until the addition of ascorbic acid was complete.

Table 1. Conditions for the preparation of cubic copper nanoparticles via seed (S) mediation

Sample set (prepared from)	$[M^0]/[M^+]$	$[M^0] + [M^+]$ (mol.dm^{-3})	Ascorbic acid (mol.dm^{-3})
A (from S)	1 : 99	2×10^{-4}	4×10^{-4}
B (from A)	1 : 8935	2×10^{-4}	4×10^{-4}
C (from B)	1 : 806360	2×10^{-4}	4×10^{-4}

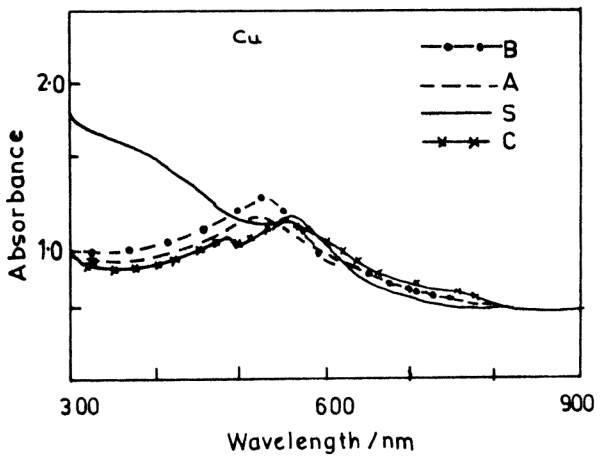

Figure 1. UV-visible spectra of copper nanoparticles of various sizes. Size increases from seed particle 'S', through 'A', 'B' to 'C'. Conditions are given in Table 1.

†For correspondence. (e-mail: tpal@chem.iitkgp.ernet.in)